

Quantum Gates Robust to Secular Amplitude Drifts

Qile David Su,* Robijn Bruinsma, and Wesley C. Campbell

Department of Physics and Astronomy, University of California, Los Angeles, CA 90095, USA

Quantum gates are typically vulnerable to imperfections in the classical control fields applied to physical qubits to drive the gates. One approach to reduce this source of error is to break the gate into parts, known as *composite pulses* (CPs), that typically leverage the constancy of the error over time to mitigate its impact on gate fidelity. Here we extend this technique to suppress *secular drifts* in Rabi frequency by regarding them as sums of *power-law drifts* whose first-order effects on over- or under-rotation of the state vector add linearly. We show that composite pulses that suppress the power-law drifts t^p for all $p \leq n$ are also high-pass filters of *filter order* $n+1$ [1]. We present sequences that satisfy our proposed *power law amplitude* PLA(n) criteria, obtained with this technique, and compare their simulated performance under time-dependent amplitude errors to some traditional composite pulse sequences. We find that there is a range of noise frequencies for which the PLA(n) sequences provide more error suppression than the traditional sequences, but in the low frequency limit, nonlinear effects become more important for gate fidelity than frequency roll-off. As a result, the previously known F_1 sequence, which is one of the two solutions to the PLA(1) criteria and furnishes suppression of both linear secular drift and the first order nonlinear effects, is a better noise filter than any of the other PLA(n) sequences in the low frequency limit.

I. INTRODUCTION

In the network model, quantum computation (QC) relies on applying quantum logic gates to qubits. In physical QC implementations, the gates are typically realized with applied classical fields (hereafter, *pulses*) that are necessarily imperfect [2–4]. Unwanted variations in the power and duration of the control pulses, for example, due to heating of the amplifier, can cause over- or under- rotations of the state vector, which we will refer to as amplitude errors. Alternatively, instability of the frequency of the pulses (or, equivalently, the energy splitting of the qubit states) causes the control pulses to stray from resonance, which we will refer to as detuning errors. These imperfections are a major obstacle to QC [5]. While quantum error correction provides a way to perform fault tolerant calculation in principle, the error probability per gate must still be reduced to less than a certain critical value, estimates for which go as low as 10^{-6} [6–9].

Since the characteristic timescale of pulse imperfections is typically long compared to the duration of the pulse, strategies to mitigate static errors (effectively, by depolarizing the error using techniques similar to spin echo) have been employed extensively in QC. It has been shown that infidelity from static amplitude and/or detuning errors can be suppressed using composite pulses [10–20]. In the case of open quantum systems undergoing linear decoherence, dynamically corrected gates can reduce the error per gate [21]. The principle behind both techniques is that by careful construction of the pulse sequence (or simply, sequence), errors accumulated earlier in a sequence are cancelled by those acquired later. Certain pulse sequences, such as the Knill sequence (5 successive π pulses with phases $30^\circ, 0^\circ, 90^\circ, 0^\circ, 30^\circ$) [22, 23] and the F_1 sequence (5 successive π pulses with phases $46.6^\circ, 255.5^\circ, 0^\circ, 104.5^\circ, 313.4^\circ$) [24], cancel the error contributed by the leading order term in the Magnus expansion of the propagator.

The Knill sequence simultaneously suppresses static amplitude and detuning errors to first order in the Magnus expansion, while the F_1 sequence suppresses static amplitude errors to second order. It has been verified both numerically and experimentally that pulse sequences designed for static errors can, to some extent, suppress errors at the low frequency end of the power spectral density [25–27]. A key concept is the pulse sequence’s *filter function*, analogous to the transfer function for electrical filters, which characterizes the frequency domain response of the infidelity of the operation achieved by the pulse sequence to the time-dependent drift experienced by the system [1, 28–31]. For example, the filter function can be shaped into a notch filter by adjusting the parameters in the sequence [32]. The behavior of the filter function near zero frequency, as determined by the dominant term in the Taylor expansion in frequency domain, has been identified as an important characteristic of the pulse sequence, especially in dynamical decoupling methods, such as Uhrig Dynamical Decoupling (UDD) protocols, which address dephasing noise [1, 29, 33, 34].

In this paper, we construct pulse sequences that suppress drifts in the amplitude of the control pulses, specifically, *secular drifts*, *i.e.*, those that occur at frequencies smaller than the Rabi frequency of the pulses. We assume that the drifts are analytic in time, thus admitting Taylor expansions into t^n *power-law drifts*. Since we intuitively expect the lowest powers of time to be the most important, we will design composite pulses that successively cancel the effect from each term in the Taylor expansion of the drift. This is different from the frequency domain expansion that we referred to in the previous paragraph, since we perform the Taylor expansion on the drift themselves in the time domain. It turns out that a pulse sequence’s response to power-law drifts is closely connected to the roll-off of its filter function near zero frequency, sometimes used to define the *filter order* [1]. While the design principle we introduce do not depend on the frequency domain behavior of the filter function, this close connection nevertheless provides further evidence that these pulse sequences may also be seen as high-pass filters. We illustrate this by calculating

* Contact at (he/him/his): qilesu@g.ucla.edu

the filter function analytically and running numerical simulations. Notably, ref. [35] adopts a time domain analysis that is similar to ours. There, the UDD protocols are justified by their ability to cancel polynomial variations in the qubit precession frequency (detuning error) with unknown coefficients. The distinction between such an analysis and the one that we are to present, apart from our focus on amplitude errors, lies in the constraints. While in dynamical decoupling, one wishes to maintain the state for some given amount of time τ , with composite pulses we have no particular constraint on the duration of the protocol, except that it be achievable with some given control strength (Rabi frequency).

The rest of this paper is organized as follows. Section II A defines quantity relevant to the problem and expresses the gate infidelity with terms in the Magnus expansion. Section II B Taylor expands a secular drift in the pulse amplitude into power-law drifts and proposes the power law amplitude PLA(n) criteria, which constrains the pulse sequence. Section II C relates suppression of power-law drifts to the low frequency roll-off of the pulse sequence. In section III A we solve the PLA(1) constraints analytically and show that the F_1 sequence is in fact one of its two distinct solutions, the other of which we label [PLA(1)]₂. In section III B we solve the PLA(n) constraints for $n > 1$ numerically. In section IV, we numerically simulate the frequency response of the sequences that satisfy the PLA(n) criteria, and compare their performance to a few known pulse sequences.

II. THEORY

A. Background

We consider a single, ideal qubit consisting of an isolated, stable, two-level system in which transitions between the two states can be induced by oscillating control fields resonant with the qubit splitting, and focus on its behavior in the presence of non-ideal control fields. More detailed background information may be found in [25, 28]. A pulse sequence is made from N simple pulses that are rotations of the qubit's state vector (Bloch vector) around single axes. Here we assume the ideal pulses have square envelopes, the rotation axes are always confined to the equatorial plane of the Bloch sphere, and there is no delay time in between pulses. The l th pulse begins at t_{l-1} and ends at t_l . The error-free control-field amplitude of pulse l (which we will identify as the Rabi frequency) is Ω_l , and its phase (which sets the rotation axis) is ϕ_l . Finally, we denote $\tau = t_N$. In the rotating frame, after suitable approximations, the error-free Hamiltonian ($\hbar \equiv 1$) is given by

$$H_0(t) = \sum_{l=1}^N G^{(l)}(t) \frac{\Omega_l}{2} \boldsymbol{\rho}_a^{(l)} \cdot \boldsymbol{\sigma}, \quad (1)$$

where we define the vectors $\boldsymbol{\rho}_a^{(l)} \equiv \boldsymbol{\rho}(\phi_l) \equiv (\cos \phi_l, \sin \phi_l, 0)$ and the square envelope function $G^{(l)}(t) \equiv 1$ for $t_{l-1} < t < t_l$ and 0 otherwise. We denote $U_0(t)$ as the unitary propagator generated by $H_0(t)$ (i.e., when errors are zero).

Now we can consider the influence of pulse imperfections by letting $\beta_a(t)$ and $\beta_d(t)$ be the amplitude and frequency errors, respectively, written in units of frequency. The full Hamiltonian is therefore

$$H(t) = \sum_{l=1}^N G^{(l)}(t) \frac{[\Omega_l + \beta_a(t)]}{2} \boldsymbol{\rho}_a^{(l)} \cdot \hat{\boldsymbol{\sigma}} + \frac{\beta_d(t)}{2} \sigma_z \quad (2)$$

$$= H_0(t) + \left[\beta_a(t) \left(\frac{1}{2} \sum_{l=1}^N G^{(l)}(t) \boldsymbol{\rho}_a^{(l)} \right) + \beta_d(t) \left(\frac{1}{2} \hat{\mathbf{z}} \right) \right] \cdot \hat{\boldsymbol{\sigma}} \quad (3)$$

$$= H_0(t) + H_{\text{err}}(t). \quad (4)$$

For unitary operations, the operational fidelity is defined as [25, 28],

$$\mathcal{F} \equiv \frac{1}{4} \left| \text{Tr} \left[U_0^\dagger(\tau) U(\tau) \right] \right|^2. \quad (5)$$

The term inside the absolute value sign is the Hilbert-Schmidt or trace inner product [36] between the ideal operator and the actual operator, effectively measuring their “overlap”. To separate the evolution due to $H_0(t)$ and $H_{\text{err}}(t)$, it is convenient to work in the *toggling frame* [15, 28, 37] (the interaction frame with respect to the errorless pulse sequence [13]) where the effective Hamiltonian is $H'(t) = U_0^\dagger(t) H_{\text{err}}(t) U_0(t)$. If we perform the Magnus expansion of the propagator in the toggling frame and then transform back to the frame co-rotating with the controls (due to convergence requirements, see section 6.1 in [28]), we can write the full propagator as the product of the error-free propagator and a correction due to $H_{\text{err}}(t)$,

$$U(\tau) = U_0(\tau) \exp [-i \mathbf{a} \cdot \hat{\boldsymbol{\sigma}}] \quad (6)$$

where $\mathbf{a} = \mathbf{a}_1 + \mathbf{a}_2 + \dots$,

$$\mathbf{a}_1 = \int_0^\tau [\beta_a(t) \boldsymbol{\rho}_a(t) + \beta_d(t) \boldsymbol{\rho}_d(t)] dt \quad (7)$$

$$\begin{aligned} \mathbf{a}_2 = & \int_0^\tau dt_1 \int_0^{t_1} dt_2 [\beta_a(t_1) \boldsymbol{\rho}_a(t_1) + \beta_d(t_1) \boldsymbol{\rho}_d(t_1)] \times \\ & [\beta_a(t_2) \boldsymbol{\rho}_a(t_2) + \beta_d(t_2) \boldsymbol{\rho}_d(t_2)] \end{aligned} \quad (8)$$

...

$\boldsymbol{\rho}_a(t)$ and $\boldsymbol{\rho}_d(t)$ are the axes around which the rotations due to the presence of error occur in the toggling frame. They are defined as,

$$\boldsymbol{\rho}_a(t) \equiv \frac{1}{2} \sum_{l=1}^N G^{(l)}(t) \boldsymbol{\rho}_a^{(l)} \Lambda^{(l-1)}, \quad (9)$$

$$\boldsymbol{\rho}_d(t) \equiv \frac{1}{2} \sum_{l=1}^N G^{(l)}(t) \boldsymbol{\rho}_d^{(l)}(t - t_{l-1}) \Lambda^{(l-1)}, \quad (10)$$

where

$$\Lambda_{ij}^{(l-1)} \equiv \frac{1}{2} \text{Tr} [R_{l-1}^{\prime \dagger} \hat{\sigma}_i R_{l-1}' \hat{\sigma}_j], \quad (11)$$

is a 3 by 3 matrix and

$$\rho_{d,j}^{(l)}(t - t_{l-1}) \equiv \frac{1}{2} \text{Tr}[U_0^\dagger(t, t_{l-1}) \sigma_z U_0(t, t_{l-1}) \sigma_j] \quad (12)$$

is a 3D row vector. R'_{l-1} and $U_0(t, t_{l-1})$ are defined as follows,

$$R'_{l-1} \equiv R_{l-1} R_{l-2} \dots R_1 \quad (13)$$

$$R_l \equiv U_0(t_l, t_{l-1}), \quad (14)$$

$$U_0(t, t_{l-1}) \equiv \exp[-i\Omega_l(t - t_{l-1}) \rho_a^{(l)} \cdot \hat{\sigma}/2]. \quad (15)$$

The derivation of $\rho_1(t)$ and $\rho_d(t)$ can be found in [28]. Because $\rho_a(t)$ and $\rho_d(t)$ depend on the parameters of the control pulse, they are also called ‘‘control vectors’’. The infidelity can be written in terms of \mathbf{a}_i ,

$$1 - \mathcal{F} = 1 - \frac{1}{4} |\text{Tr}[\exp(-i\mathbf{a} \cdot \hat{\sigma})]|^2 = 1 - \cos^2(|\mathbf{a}|) \quad (16)$$

$$= |\mathbf{a}|^2 - \frac{1}{3} |\mathbf{a}|^4 + \dots \quad (17)$$

$$= (\mathbf{a}_1 + \mathbf{a}_2 + \mathbf{a}_3 + \dots)^2 - \frac{1}{3} [(\mathbf{a}_1 + \mathbf{a}_2 + \mathbf{a}_3 + \dots)^2]^2 + \dots \quad (18)$$

$$= |\mathbf{a}_1|^2 + (2\mathbf{a}_1 \cdot \mathbf{a}_2) + \left(\mathbf{a}_2^2 - \frac{1}{3} |\mathbf{a}_1|^4 + 2\mathbf{a}_1 \cdot \mathbf{a}_3 \right) + \dots \quad (19)$$

In the limit of small errors, better fidelity is achieved by successively zeroing $\mathbf{a}_1, \mathbf{a}_2$, etc. When the magnitudes of $\beta_a(t)$ and $\beta_d(t)$ are small, zeroing \mathbf{a}_1 may be sufficient.

Our analysis within this section will be done in the linear response regime where \mathbf{a}_1 dominates, so we may write

$$1 - \mathcal{F} \approx |\mathbf{a}_1|^2. \quad (20)$$

In addition, from here onward we will set $\beta_d(t) = 0$, restricting ourselves to amplitude errors only. The errorless Rabi frequency Ω will be a constant.

B. Secular drifts

In real devices, time-dependent imperfections in pulse amplitude (or, more generally, pulse area) can occur, for instance due to the temperatures of components changing during uneven use [5, 38]. To model this, we let $\beta_a(t)$ describe a secular drift, *i.e.*, a drift whose characteristic timescale is much longer than a pulse. We assume that $\beta_a(t)$ is analytic, so it can be expressed as a power series in time,

$$\beta_a(t) = \sum_{p=0}^{\infty} \frac{1}{p!} \beta_a^{(p)} t^p. \quad (21)$$

Plugging it into Eq.(7),

$$\mathbf{a}_1 = \sum_{p=0}^{\infty} \beta_a^{(p)} \mathbf{c}_{a,p}, \quad (22)$$

where

$$\mathbf{c}_{a,p} \equiv \frac{1}{p!} \int_0^\tau t^p \rho_a(t) dt. \quad (23)$$

To suppress a secular drift up to and including a power-law t^n dependence, the task is to design $\rho_a(t)$ such that the following is satisfied:

$$\mathbf{c}_{a,p} = 0 \quad \text{for } p = 0, 1, \dots, n. \quad (24)$$

When this is achieved, the infidelity is, to leading order,

$$1 - \mathcal{F} \approx |\mathbf{a}_1|^2 \approx \left(\beta_a^{(n+1)} \right)^2 (\mathbf{c}_{a,n+1})^2. \quad (25)$$

As n increases, we suppress more terms in the infidelity within the linear regime, but the length of the sequences necessary to satisfy the constraints also increases. A longer pulse sequence experiences the error for a longer period of time, which manifests in the next unconstrained $\mathbf{c}_{a,p}$. This puts a practical limit on n .

Now we write Eq.(24) in terms of parameters of a composite pulse requires knowledge of its possible forms. In general, the net effect of composite pulse changes wildly when the parameters of each of the constituent pulses are allowed to vary. For this reason, we choose to focus on pulse sequences that perform a net π -pulse around the x -axis (an \hat{X} gate) in this work. Such a choice (as opposed to, say, a $\pi/2$ - or $\pi/4$ -pulse) leads to simplified sequences because the target gate can always be constructed from an odd number of π -pulses whose phases can be freely varied without compromising the target \hat{X} gate. The form for the composite pulse sequence will be

$$\pi_{\phi_1} \rightarrow \pi_{\phi_2} \rightarrow \dots \rightarrow \pi_{\phi_N} \quad (N \text{ is odd}), \quad (26)$$

where the notation π_{ϕ_l} means a π -pulse with phase ϕ_l , and ϕ_l are constraint by the following condition to ensure an \hat{X} gate,

$$g(\phi) \equiv \sum_{l=1}^N (-1)^l \phi_l = k\pi \quad \text{for integer } k. \quad (27)$$

One may check that this sequence indeed accomplishes an \hat{X} gate by verifying that the error-free propagator is $U_0(\tau) = \pm \exp[-i\pi\hat{\sigma}_x/2]$. An overall phase offset for all pulses can be chosen to satisfy Eq.(27), and one may verify that it does not affect the constraints that we establish later. For a construction that accommodate some gates other than the \hat{X} gate, with similar flexibility, see [5, 12] where the target gate is prepended or appended with compensating π -pulses.

Next, we use Eq.(9) to write the constraints explicitly in terms of ϕ_l . The term $\Lambda^{(l-1)}$ in Eq.(9) is the transformation matrix from the original frame to the toggling frame during the $(l-1)$ th pulse. Under the composite pulse assumed in Eq.(26), we have $t_{l-1} = (l-1)\pi/\Omega$ and

$$\rho_a^{(l)} \Lambda^{(l-1)} = \rho(\phi'_l) = (\cos \phi'_l, \sin \phi'_l, 0), \quad (28)$$

where ϕ'_j are the *toggling-frame phases* [16],

$$\phi'_j \equiv -(-1)^j \phi_j - \sum_{k=1}^{j-1} (-1)^k 2\phi_k. \quad (29)$$

Then Eq.(23) simplifies to

$$\mathbf{c}_{a,p} = \frac{1}{2p!} \sum_{l=1}^N \boldsymbol{\rho}(\phi'_l) \int_{t_{l-1}}^{t_l} t^p dt \quad (30)$$

$$= \frac{1}{2} \left(\frac{\pi}{\Omega} \right)^{p+1} \frac{1}{(p+1)!} \sum_{l=1}^N \boldsymbol{\rho}(\phi'_l) [l^{p+1} - (l-1)^{p+1}] \quad (31)$$

$$= \frac{1}{2} \left(\frac{\pi}{\Omega} \right)^{p+1} \sum_{q=0}^p \frac{1}{q!(p-q+1)!} \mathbf{c}'_{a,q}. \quad (32)$$

where we use the binomial theorem and define

$$\mathbf{c}'_{a,p} \equiv \sum_{l=1}^N (l-1)^p \boldsymbol{\rho}(\phi'_l). \quad (33)$$

Therefore the constraints in Eq.(24) is equivalent to

$$\mathbf{c}'_{a,p} = 0 \quad \text{for } p = 0, 1, \dots, n. \quad (34)$$

$\mathbf{c}'_{a,p}$ has a simpler form than $\mathbf{c}_{a,p}$ as well as a straightforward interpretation: in the toggling frame, the rotation vectors weighted by the p th power of the pulse number must sum to zero. We label Eq.(34) and Eq.(27) as the power law amplitude PLA(n) criteria. They will be solved in section III. Solutions will be labeled $[\text{PLA}(n)]_i$, where i is an integer index which differentiates distinct solutions.

C. Random errors

In this section we examine the case of random errors. Following [25, 28], suppose the amplitude error $\beta_a(t)$ is a stationary process and possesses zero mean and an auto-covariance function defined by $R_a(t) = \langle \beta_a(t_0) \beta_a(t_0 + t) \rangle$. The power spectral density of the amplitude imperfection term is

$$S_a(f) \equiv \int_{-\infty}^{\infty} R_a(t) e^{-i2\pi f t} dt. \quad (35)$$

In practice, the fidelity is measured by repeating the experiment many times, so we should average the infidelity from Eq.(19) over the noise ensemble. Using Eq.(7) to rewrite the dominant term in the infidelity (Eq. (20)) with frequency domain variables, we get

$$1 - \langle \mathcal{F} \rangle \approx \langle |\mathbf{a}_1|^2 \rangle = \int_{-\infty}^{\infty} df \frac{1}{(2\pi f)^2} S_a(f) h_a(f), \quad (36)$$

where $h_a(f)$, the *filter function* [25, 28], is given by

$$h_a(f) \equiv \tilde{\boldsymbol{\rho}}_a^*(f) \cdot \tilde{\boldsymbol{\rho}}_a(f), \quad (37)$$

and

$$\tilde{\boldsymbol{\rho}}_a(f) \equiv -i2\pi f \int_0^{\tau} \boldsymbol{\rho}_a(t) e^{i2\pi f t} dt. \quad (38)$$

To suppress low frequency errors, it is desirable for the filter function to have a steep roll-off in the low frequency limit. The low frequency behavior of the filter function is captured by its Taylor series expansion at $f = 0$. Supplemental materials on the filter function in the low frequency regime shows that, if Eq.(24) is satisfied, then the leading order term of the filter function in the low frequency limit is

$$h_a(f) \approx (\mathbf{c}_{a,n+1})^2 (2\pi f)^{2n+4}. \quad (39)$$

Thus, if a pulse sequence suppresses power-law drifts, it automatically suppresses low frequency errors in the regime of linear response.

III. SOLVING THE CONSTRAINTS

In this section we solve the PLA(n) constraints for the parameters ϕ_l . The precise mathematical problem we attempt to solve is restated as follows. For a given n , we choose an sequence length N (an odd integer) and seek a sequence $\phi_1, \phi_2, \dots, \phi_N$ that satisfies Eq.(27) and

$$\mathbf{c}'_{a,p} = \sum_{l=1}^N (l-1)^p \boldsymbol{\rho}(\phi'_l) = 0 \quad \text{for } p = 0, 1, \dots, n \quad (40)$$

where ϕ'_l are the toggling-frame phases previously defined, and $\boldsymbol{\rho}(\phi'_l) \equiv (\cos \phi'_l, \sin \phi'_l, 0)$.

From the definition of $\boldsymbol{\rho}(\phi'_l)$, the z -components of Eqs.(40) are always 0, so we can swap the xy -plane for the complex plane to make the notation more succinct,

$$\sum_{l=1}^N (l-1)^p e^{i\phi'_l} = 0 \quad \text{for } p = 0, 1, \dots, n. \quad (41)$$

The transformation between ϕ'_l and ϕ_l is invertible, so we solve for ϕ'_l and convert them to ϕ_l afterwards. Trial and error suggests that the general solution of the Eqs.(41) is quite non-trivial. For a given n , Eqs.(41) specifies $(2n+2)$ real constraints. We anticipate the need for $(2n+2)$ degrees of freedom to solve them. Since the length N must be odd, we anticipate that $N \geq 2n+3$. It has been shown that the Weierstrass substitution $\tan(\phi_l/2) = t_l$ converts transcendental equations such as Eqs.(41) into a system of polynomial equations that may be solved with the method of Gröbner basis [12]. However, for small n and N , elementary algebra is sufficient to obtain analytical solutions. For larger n and N , numerical solutions may be attempted.

A. Analytically: $n = 1$

When $n = 0$, the constraints only concern the ability of the composite pulse to suppress constant errors. To produce a composite pulse that suppresses time-dependent errors, we start with $n = 1$, *i.e.*, the PLA(1) criteria and attempt a solution with $N = 5$. After making linear combinations of

Eqs.(40), we can obtain two new constraints that are symmetric about the center pulse,

$$e^{i\phi'_1} + e^{i\phi'_2} + 1 + e^{i\phi'_4} + e^{i\phi'_5} = 0 \quad (42)$$

$$-2e^{i\phi'_1} - e^{i\phi'_2} + e^{i\phi'_4} + 2e^{i\phi'_5} = 0, \quad (43)$$

where we have set $\phi'_3 = 0$ without loss of generality. Limiting the domains phases to $-\pi < \phi'_l \leq \pi$ and applying Euler's identity yields

$$1 + 2e^{i\alpha} \cos \beta + 2e^{i\gamma} \cos \delta = 0 \quad (44)$$

$$4ie^{i\alpha} \sin \beta + 2ie^{i\gamma} \sin \delta = 0, \quad (45)$$

where we define

$$\alpha \equiv \frac{\phi'_5 + \phi'_1}{2}, \quad \beta \equiv \frac{\phi'_5 - \phi'_1}{2}, \quad (46)$$

$$\gamma \equiv \frac{\phi'_4 + \phi'_2}{2}, \quad \delta \equiv \frac{\phi'_4 - \phi'_2}{2}, \quad (47)$$

The newly defined angles have ranges $\alpha, \gamma \in (-\pi, \pi]$, and $\beta, \delta \in (-\pi, \pi)$.

First, we consider case A: $\sin \beta \neq 0$. From Eq.(45),

$$e^{i\alpha} = -\frac{\sin \delta}{2 \sin \beta} e^{i\gamma}. \quad (48)$$

From here we deduce that $\sin \delta = \pm 2 \sin \beta \neq 0$ and that $\beta, \delta \neq 0$. Since $\phi'_1 = \alpha - \beta \leq \pi$, $\phi'_5 = \alpha + \beta \leq \pi$, and $\beta \neq 0$, we must have $\alpha \neq \pi$. Similarly $\gamma \neq \pi$.

One can check that the case $\sin \delta = 2 \sin \beta$ leads to a contradiction. Therefore $\sin \delta = -2 \sin \beta$. Then $e^{i\alpha} = e^{i\gamma}$, i.e., $\alpha = \gamma$. Plugging this in to Eq.(44), we get

$$1 = -2(\cos \beta + \cos \delta) e^{i\alpha}. \quad (49)$$

We have that $\alpha = \gamma = 0$, and $\cos \beta + \cos \delta = -\frac{1}{2}$. With trigonometric identities and substitution, we obtain that the solutions to the equations

$$\cos \beta + \cos \delta = -\frac{1}{2} \quad (50)$$

$$\sin \delta = -2 \sin \beta \quad (51)$$

are $\beta = \pm \arccos\left(\frac{1-2\sqrt{10}}{6}\right)$, $\delta = \mp \arccos\left(\frac{-2+\sqrt{10}}{3}\right)$. Thus,

$$\phi'_1 = -\phi'_5 = -\beta, \quad (52)$$

$$\phi'_2 = -\phi'_4 = -\delta. \quad (53)$$

Using Eq.(29), we can convert these phases back to the original frame. After adding an appropriate phase offset, we get

$$\phi = (-\beta, -2\beta + \delta, -2\beta + 2\delta, -2\beta + \delta, -\beta). \quad (54)$$

We label this solution the $[\text{PLA}(1)]_2$ sequence. We will see that the other solution ($[\text{PLA}(1)]_1$, from case B below) is a well known sequence.

Now consider case B: $\sin \beta = 0$. Then from Eq.(45), $\beta = \delta = 0$. Plugging into Eq.(44),

$$1 + 2e^{i\alpha} + 2e^{i\gamma} = 0. \quad (55)$$

By drawing a triangle with side lengths 1, 2, and 2, it can be readily obtained that $\alpha = -\gamma = \pm \arccos\left(-\frac{1}{4}\right)$. So

$$\phi'_1 = -\phi'_2 = -\phi'_4 = \phi'_5 = \alpha. \quad (56)$$

Again using Eq.(29), we can convert these phases back to the original frame,

$$\phi = (-3\alpha, -\alpha, 0, \alpha, 3\alpha). \quad (57)$$

This sequence, which would here nominally be denoted $[\text{PLA}(1)]_1$, is in fact the well known F_1 sequence discovered by Wimperis [14, 24]. It is time-symmetric in the toggling frame because $\phi'_j = \phi'_{6-j}$. Consequently, $\rho_a(t) = \rho_a(\tau - t)$. If we shift the origin of time to the middle of the sequence, then $\rho_a(t) = \rho_a(-t)$. Incidentally, with this symmetry, the constraints $\mathbf{c}_{a,p}$ evaluate to 0 for all odd power-law drifts,

$$\mathbf{c}_{a,p} = \frac{1}{p!} \int_{-\tau/2}^{\tau/2} t^p \rho_a(t) dt = 0 \text{ if } p \text{ is odd.} \quad (58)$$

B. Numerically $n > 1$

When $n > 1$ and N becomes relatively large, exact solution becomes intractable, and we can attempt to solve the constraints Eq.(24) and Eqs.(40) numerically. Given n , we can choose an appropriate sequence length N and define the objective function in terms of the original phases ϕ_l ,

$$U(\phi) = \sin^2[g(\phi)] + \sum_{p=0}^n |\mathbf{c}'_{a,p}(\phi)|^2. \quad (59)$$

(We exploit the fact that the sine function has zeros at $g(\phi) = k\pi$ and both terms in Eq. (59) are non-negative.) The objective function is minimized to 0 when the constraints are satisfied. When implementing this objective function in code, it helps to scale each term in $U(\phi)$ so that their magnitudes are similar over the domain. A random initial guess may be chosen and a minimization algorithm can be employed to find the optimum ϕ . If the algorithm terminates at $U(\phi) = 0$, then we have found a solution to the constraints given n for N . Otherwise a different initial guess or a larger N may be chosen and the procedure repeated. In general, for each n we are interested in finding the shortest sequence that can satisfy the constraints. When N is too small however, a solution may not be found. Since the numerical procedure previously described does not differentiate the non-existence of solutions from unfortunate initial guesses, the shortest sequences we do only provide an upper bound for the sequence length N , and even shorter sequences may exist that satisfy the constraints.

Phases	$[\text{PLA}(2)]_1$	$[\text{PLA}(3)]_1$
ϕ_1	1.76715945118259	4.83865251534654
ϕ_2	5.41431157276639	1.84379790507494
ϕ_3	0.60338726707880	1.93262975911420
ϕ_4	2.25267362096692	0.48888316408261
ϕ_5	5.66568802156378	3.13701277837872
ϕ_6	0.11541193070770	3.67903366892586
ϕ_7	2.91932560661088	3.52519916847217
ϕ_8	3.75846738675240	5.73340443857318
ϕ_9	0.58530416475736	4.41388024396790
ϕ_{10}		4.49690511625724
ϕ_{11}		1.53624248122411

TABLE I. Instances of numerical solutions for PLA(2) and PLA(3). Since the numerical procedure that was used to generate these sequences started with a random initial guess, there can be other solutions that are not listed here.

IV. BEYOND LINEAR RESPONSE

In section II B, we showed that to first order in the Magnus expansion, the sequences we constructed filter out low frequencies. However, the true infidelity (Eq.(19)) contains higher order terms. We expect that in the low frequency regime, termed the “DC limit” in [25], the second order term \mathbf{a}_2 , which was not accounted for by the filter function, should dominate the infidelity, *i.e.*, $1 - \mathcal{F} \approx |\mathbf{a}_2|^2$. To examine this effect, we use a Monte Carlo simulation to compute the true infidelity of the composite pulses under random amplitude errors. If we choose the power spectral density of the errors to be narrow-band and centered around f_c , then we may scan f_c to numerically obtain the frequency response of the composite pulses. See supplemental materials for details about the Monte Carlo simulation.

Figure 1 shows the simulated frequency response of a number of composite pulses. We elaborate on the derivation of the theory curves that are present in the figure. For narrow-band errors centered around the frequency f_c , Eq.(20) says that to first order, the infidelity is approximately

$$1 - \langle \mathcal{F} \rangle \approx \langle |\mathbf{a}_1|^2 \rangle = \int_{-\infty}^{\infty} df \frac{1}{(2\pi f)^2} S_a(f) h_a(f) \quad (60)$$

$$\approx \frac{1}{(2\pi f_c)^2} h_a(f_c) \int_{-\infty}^{\infty} df S_a(f), \quad (61)$$

where $\int_{-\infty}^{\infty} df S_a(f) = \sigma_{\beta}^2$ is the square of the RMS error. To improve the accuracy of the theory curve, we add in the contribution from the second order term in the Magnus expansion. From Eq.(8),

$$\mathbf{a}_2 = \int_0^{\tau} dt_1 \int_0^{t_1} dt_2 \beta_a(t_1) \beta_a(t_2) \rho_a(t_1) \times \rho_a(t_2). \quad (62)$$

The second order term in the Magnus expansion is only important in the low frequency regime, so it suffices to take the limit $f \rightarrow 0$ and let $\beta_a(t) = \beta_a$ be a constant over time [25].

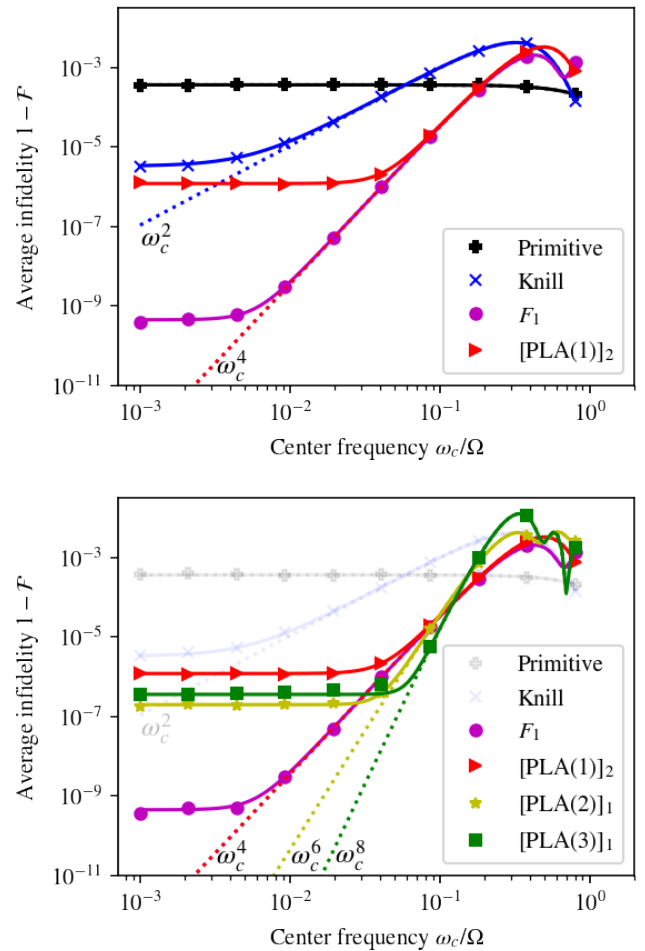


FIG. 1. Simulated frequency response of pulse sequences for amplitude errors. The plots are grouped into two figures for legibility and ease of comparison. On the horizontal axis, $\omega_c = 2\pi f_c$ and $\Omega = 1.5 \times 10^6$ rad/s is the Rabi frequency. The ratio of RMS amplitude error and the Rabi frequency is 1.21×10^{-2} . Dots: average infidelity of a composite pulse obtained by Monte Carlo simulation. Dashed curves: infidelity predicted by the filter function (Eq.(61)). Solid curves: infidelity prediction that includes terms in the Magnus expansion to the third order (Eq.(61) + Eq. (65) + third order correction derived analogously).

We may write

$$\mathbf{a}_{2,DC} = \beta_a^2 \int_0^{\tau} dt_1 \int_0^{t_1} dt_2 \rho_a(t_1) \times \rho_a(t_2). \quad (63)$$

$\rho_a(t)$ is a piecewise constant function. By cutting the integral into segments with constant integrand and substituting the definition of $\rho_a(t)$, we may eventually arrive at

$$\mathbf{a}_{2,DC} = \frac{1}{4} \left(\frac{\pi}{\Omega} \right)^2 \beta_a^2 \sum_{l=1}^N \sum_{m=1}^{l-1} \sin(\phi'_m - \phi'_l) \hat{\mathbf{z}}, \quad (64)$$

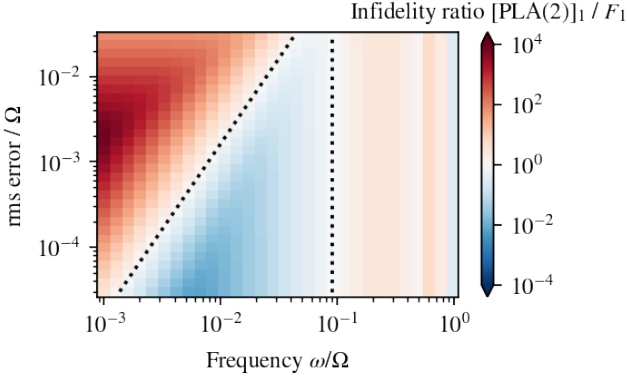


FIG. 2. Effect of the RMS error on the $[\text{PLA}(2)]_1$ performance bandwidth. Plotted in color is the infidelity ratio between $[\text{PLA}(2)]_1$ and F_1 , calculated using the third-order corrected theory curves (solid curves in figure 1). The blue region indicates the parameters for which $[\text{PLA}(2)]_1$ performs better than F_1 . A similar shaped blue region exists for $[\text{PLA}(3)]_1$. For the $[\text{PLA}(1)]_2$ sequence however, there is no parameter range over which it does better than F_1 . The dashed lines show the boundaries of the blue region: $(\frac{\omega}{\Omega})^2 > \frac{\sigma_\beta}{\Omega} (\Omega^3 |\mathbf{c}_{a,2}|)^{-1} \frac{\sqrt{3}}{4} \pi^2 \left| \sum_{l=1}^N \sum_{m=1}^{l-1} \sin(\phi'_m - \phi'_l) \right|$, and $\frac{\omega}{\Omega} < \frac{|\Omega^3 \mathbf{c}_{a,2}|}{|\Omega^4 \mathbf{c}_{a,3}|}$, where σ_β is the RMS error, $\mathbf{c}_{a,2}$ is calculated for the F_1 sequence, and $\mathbf{c}_{a,3}$ and ϕ'_l is calculated for the $[\text{PLA}(2)]_1$ sequence (See supplemental materials for derivation of the boundary of regimes).

whose squared average is

$$\langle |\mathbf{a}_{2,\text{DC}}|^2 \rangle = \frac{1}{16} \left(\frac{\pi}{\Omega} \right)^4 \langle \beta_a^4 \rangle \left[\sum_{l=1}^N \sum_{m=1}^{l-1} \sin(\phi'_m - \phi'_l) \right]^2. \quad (65)$$

If β_a follows a Gaussian distribution, then $\langle \beta_a^4 \rangle = 3\sigma_\beta^4$. Therefore we may assemble a more accurate prediction of the infidelity of a composite pulse for low frequency amplitude errors by summing the contribution from the filter function and the second order Magnus term. The third order correction can be derived analogously.

Figure 1 shows that the summed theory curves explain the simulated performance of the composite pulses with significant accuracy. The slope of the filter function shows that, to first order, sequences that satisfy the $\text{PLA}(n)$ criteria become increasingly better high-pass filters with increasing n . A notable exception is that the second order term in the Magnus expansion vanishes for the F_1 sequence, which explains the discrepancy between its theory curve and simulated data [24]. This can also be seen from the fact that it has zero area in the toggling frame (see section V of [39]), hence its excellent performance compared to other composite pulses. Its DC limit results in turn from the third order Magnus term, which may be readily computed.

The Knill sequence, the F_1 sequence, and the $\text{PLA}(1)$ sequence are all composed from five π pulses. Each has 4 degrees of freedom after subtracting a global shift of the phases. For the Knill sequence, first-order suppression of constant

amplitude and detuning errors establishes two simultaneous constraints on the phases of the pulse [23, 39]. For F_1 and $\text{PLA}(1)$, the detuning constraint is swapped out for first-order suppression of linearly-varying amplitude errors. Hence in Figure 1, the filter function for F_1 and $\text{PLA}(1)$ have steeper slopes. Although the F_1 sequence and the $\text{PLA}(1)$ sequence result from the same set of constraints (see section III A), the F_1 sequence additionally provides second-order suppression of constant amplitude error. Hence the F_1 sequence performs better in the low frequency limit than $\text{PLA}(1)$. Figure 2 shows the regime over which one might prefer the $[\text{PLA}(1)]_2$ sequence over the F_1 sequence and vice versa. With decreasing RMS error, the contribution from the second order Magnus term drops out from the infidelity, allowing the frequency response to be dominated by the constant roll-off predicted by first order analysis over a wider bandwidth.

V. CONCLUSION

In summary, we have developed criteria for designing pulse sequences for single-qubit quantum gates that can suppress, within linear response, errors from pulse amplitude imperfections due to time-dependent secular drifts in experimental instruments. Specifically, we found analytically that there are only two five pulses sequences, $[\text{PLA}(1)]_2$ and the F_1 sequence due to Wimperis [24], that suppress static error and linear drift to first order in the Magnus expansion. Of the two sequences, F_1 is better for suppressing low frequency errors in the limit of small errors. Since most well known composite pulses are designed for static errors, they do not suppress power-law drifts, such as t^n for $n \geq 1$, in the pulse amplitude, *i.e.*, they do not satisfy the $\text{PLA}(n)$ criteria. The well known Knill sequence which simultaneously suppresses static amplitude and detuning errors [22, 23] performs poorly for linear drift. An exception is Wimperis's F_1 sequence, which obeys the $\text{PLA}(1)$ criteria. Generalizing beyond linear drift, we explicitly constructed, up to $n = 3$, instances of sequences that satisfy the $\text{PLA}(n)$ criteria, which suppress power-law drifts up to t^n in the pulse amplitude. We find that these function effectively as high-pass filters of filter order $n + 1$. In figure 2 we showed that while in the low frequency limit the F_1 sequence has a lower infidelity, the sequences that satisfy the $\text{PLA}(n)$ criteria for $n > 1$ perform better than F_1 over a frequency bandwidth which widens as the error amplitude decreases. Therefore the choice of which sequence to use should include a noise model from the actual system to find the best way to suppress errors, evidencing the need for noise characterization [40, 41]. The origin of the F_1 sequence's exceptional performance is that, for static errors, it suppresses not just the linear response, but also the second order term in the error Magnus expansion, which becomes the dominant contributor to the infidelity in the low frequency limit. In fact, every sequence that is time-symmetric in the toggling frame will suppress linear drift. We conclude that suppression of the second order term is important in the low frequency regime.

The analysis is limited by the assumption of analytical drifts, so it does not extend to jumps or zigzags in the pulse

amplitude. Next, we assumed that the control pulses have square envelopes. A similar analysis may be done with non-square pulses, but analytical solutions might no longer be possible. Further, since in general one wants to use the shortest possible sequence that suppresses power-law drifts, we are interested in minimizing the sequence length. However, the random initial guess taken by the numerical procedure that we used to solve the constraint equations means that we can not eliminate the existence of shorter sequences than those we found that satisfy the same constraints. In addition, the assumption of Gaussian error distribution means that adjustments are necessary to adopt the analysis for non-Gaussian distributions. Finally, the non-linearity of the composition of rotations can cause mixing between different frequency components that is not captured by our numerical simulation, where we only inject noise of a very narrow-band.

Future work may expand the suppression of power-law drift to higher order terms in the Magnus expansion, as well as design composite pulses that address frequency detuning errors. For the first objective, cross terms will need to be examined that combine different power-law drifts and the extent to which this affects the ability to suppress each drift separately should be investigated. In addition, simultaneous expansion with respect to time and the error size means that care should be taken to order the terms in the series correctly so as to justify the truncation of the expansion. When establishing the constraints, it may reduce problem complexity to only impose a judicious selection of all relevant constraints and let the correlation between constraints help suppress the rest. It remains to be seen how the increase in the number of constraints and the sequence length changes the sensitivity of the infidelity to the most dominant term that is neglected.

For detuning errors, it may be possible to apply the analysis presented in this paper to design sequences that satisfy the Power Law Frequency (PLF(n)) criteria. It isn't obvious how to construct symmetric sequences for detuning errors in the toggling frame. A key question is how well the PLF sequences, produced in an analogous way as the PLA sequences, will compare to previous work that has been done on this subject. For example, the Knill sequence suppresses the first order term in the Magnus expansion for static detuning errors, and by strategic choice of a free parameter in the Knill sequence, it can suppress the second order term as well [39]. Although the goal of this investigation has been suppressing control errors, the similarity between the effect of instabilities in the frequency of the control pulse and that of an environment which causes the qubit splitting to fluctuate (ref. [3]) invites a consideration of previous work that aims at suppressing decoherence or dephasing [29, 30, 42] as well as control noise [1], even though some of the sequences presented there do not accomplish a non-trivial gate. Given the correspondence between power-law drift and filter function roll-off that we derived for amplitude error, there may be a similar correspondence that will unite the PLF(n) sequences, rooted in power-law drifts in the time domain, with the sequences in the referenced work. More recently, the case of non-stationary noise was investigated with a generalized notion of filter functions, that are based on the mathematical notion of frames, of which

the usual frequency domain representation of the noise spectrum is a special case [43]. Due to the framework's reported capability to handle non-stationary noise, it would be interesting to investigate the properties of the sequences presented in our paper, designed for such divergent time dependence as power-law drifts, within this framework.

VI. ACKNOWLEDGEMENTS

We would like to thank K. R. Brown, M. J. Biercuk, L. Viola, and I. L. Chuang for feedback on the draft and helpful discussions. Work on this project was carried out with support from the Lau family and Ms. Evers-Manly through the UCLA Undergraduate Research Scholars Program, the US National Science Foundation Award No. PHY-1912555, and the NSF QLCI program through grant number OMA-2016245. Initial work on this project was carried out by Xingchen Fan and Clementine Domine with support from the NSF-DMR under CMMT Grant 1836404.

VII. SUPPLEMENTAL MATERIAL

A. Filter function in the low frequency limit

We will show that if a pulse sequence suppresses power-law drifts, then it will act as a high-pass filter. The definition of the filter function is

$$h_a(f) = \tilde{\rho}_a^*(f) \cdot \tilde{\rho}_a(f), \quad (66)$$

where

$$\tilde{\rho}_a(f) = -i2\pi f \int_0^\tau \rho_a(t) e^{i2\pi f t} dt. \quad (67)$$

Plugging in gives

$$h_a(f) = (2\pi f)^2 \int_0^\tau \int_0^\tau \rho_a^*(t_1) \cdot \rho_a(t_2) e^{i2\pi f(t_2 - t_1)} dt_1 dt_2. \quad (68)$$

The complex conjugate can be omitted since $\rho_a(t)$ is real. $h_a(f)$ is real valued by definition, so we take its real part,

$$h_a(f) = (2\pi f)^2 \int_0^\tau \int_0^\tau \rho_a(t_1) \cdot \rho_a(t_2) \cdot \cos[2\pi f(t_2 - t_1)] dt_1 dt_2 \quad (69)$$

$$= \sum_{n'=0}^{\infty} \frac{(-1)^{n'}}{(2n')!} (2\pi f)^{2n'+2} \int_0^\tau \int_0^\tau \rho_a(t_1) \cdot \rho_a(t_2) \cdot (t_2 - t_1)^{2n'} dt_1 dt_2. \quad (70)$$

The last equality sign invokes the Taylor expansion of cosine. In the low frequency limit ($f \rightarrow 0$), the $n' = 0$ term domi-

nates, so

$$h_a(f) \approx (2\pi f)^2 \int_0^\tau \int_0^\tau \rho_a(t_1) \cdot \rho_a(t_2) dt_1 dt_2 \quad (71)$$

$$= (2\pi f)^2 \left(\int_0^\tau \rho_a(t) dt \right)^2. \quad (72)$$

This term vanishes if $\int_0^\tau \rho_a(t) dt = 0$. The next dominant term scales as f^4 , making the $h_a(f)$ a better high-pass filter. In general, we apply the binomial expansion to $(t_2 - t_1)^{2n'}$ in (70),

$$h_a(f) = \sum_{n'=0}^{\infty} \sum_{m=0}^{2n'} \frac{(-1)^{n'+m}}{2n'!} m!(2n' - m)! \binom{2n'}{m} \cdot (\mathbf{c}_{a,m} \cdot \mathbf{c}_{a,2n'-m}) (2\pi f)^{2n'+2}, \quad (73)$$

where, as in the section ‘‘Beyond linear response’’ in the main text,

$$\mathbf{c}_{a,p} \equiv \frac{1}{p!} \int_0^\tau t^p \rho_a(t) dt. \quad (74)$$

If Eq.(23) in the main text is satisfied, then the limits of summation can be narrowed,

$$h_a(f) = \sum_{n'=n+1}^{\infty} \sum_{m=n+1}^{2n'-n-1} \frac{(-1)^{n'+m}}{2n'!} m!(2n' - m)! \binom{2n'}{m} \cdot (\mathbf{c}_{a,m} \cdot \mathbf{c}_{a,2n'-m}) (2\pi f)^{2n'+2}. \quad (75)$$

Its leading term is $n' = n + 1$, which simplifies to

$$h_a(f) \approx (\mathbf{c}_{a,n+1})^2 \omega^{2n+4} \quad (76)$$

This quantifies the degree to which composite pulses suppress low frequency noise in the limit that only the first term in the Magnus expansion is needed.

B. Details about the Monte Carlo simulation

In the Monte Carlo simulation, we discretize the time domain and integrate the equation of motion of the qubit with the Euler method over an ensemble of numerically generated errors. At the end, we take the ensemble average of the fidelity as defined in Eq.(5). Given a power spectral density, a member of the error ensemble is generated by first dividing the frequency domain into bins f_k with width Δf and generating one complex Fourier coefficient A_k for each. If the one-sided power spectral density is $S(f)$, then the coefficients are drawn from independent Gaussian distributions,

$$\text{Re}[A_k], \text{Im}[A_k] \sim \frac{1}{2} \sqrt{S(f_k) \Delta f} N(0, 1) \quad \text{if } f_k \neq 0, \quad (77)$$

$$\text{Re}[A_k] \sim \sqrt{S(f_k) \Delta f} N(0, 1), \text{Im}[A_k] = 0 \quad \text{if } f_k = 0. \quad (78)$$

We then take the inverse Fourier transform to obtain the error in the time domain,

$$\beta(t) = A_0 + \sum_k [A_k \exp(i2\pi f_k t) + \text{c.c.}], \quad (79)$$

where A_0 is the Fourier coefficient for $f = 0$, and c.c denotes the complex conjugate. Consequently, the error has a Gaussian distribution. Here we use the following simple narrow-band (one-sided) power spectral density for the simulation,

$$S(f) = \begin{cases} A & \text{if } f \in (f_c - f_{\text{band}}/2, f_c + f_{\text{band}}/2) \\ 0 & \text{otherwise} \end{cases} \quad (80)$$

where A is chosen so that the errors have some known rms value, and f_{band} is chosen to be 2 Hz, which is sufficiently narrow.

C. Boundary of regimes

In the frequency regime, we can approximate the infidelity of the F_1 sequence by

$$1 - \langle \mathcal{F} \rangle \approx \frac{1}{(2\pi f)^2} h_a(f) \sigma_\beta^2 \quad (81)$$

$$\approx \frac{1}{(2\pi f)^2} \mathbf{c}_{a,n+1}^2 (2\pi f)^{2n+4} \sigma_\beta^2, \quad (82)$$

where σ_β is the RMS error. Since F_1 is a solution to the PLA(1) criteria, we have that $n = 1$. Plugging in,

$$1 - \langle \mathcal{F} \rangle \approx \mathbf{c}_{a,2}^2 (2\pi f)^4 \sigma_\beta^2 \quad (83)$$

In the low frequency regime, the infidelity of [PLA(2)]₁ is dominated by the second order term in the Magnus expansion. Therefore, assuming Gaussian errors, it infidelity is

$$1 - \langle \mathcal{F} \rangle \approx \langle |\mathbf{a}_{2,\text{DC}}^2| \rangle \quad (84)$$

$$= \frac{3}{16} \left(\frac{\pi}{\Omega} \right)^4 \sigma_\beta^4 \left[\sum_{l=1}^N \sum_{m=1}^{l-1} \sin(\phi'_m - \phi'_l) \right]^2, \quad (85)$$

where σ'_l are its phases in the toggling frame. At slightly larger frequencies, the infidelity of [PLA(2)]₁ is dominated by the first order term in the magnus expansion. Since for [PLA(2)]₁, we have that $n = 2$. Its infidelity is

$$1 - \langle \mathcal{F} \rangle \approx \frac{1}{(2\pi f)^2} h_a(f) \sigma_\beta^2 \quad (86)$$

$$\approx \frac{1}{(2\pi f)^2} \mathbf{c}_{a,n+1}^2 (2\pi f)^{2n+4} \sigma_\beta^2 \quad (87)$$

$$= \mathbf{c}_{a,3}^2 (2\pi f)^6 \sigma_\beta^2 \quad (88)$$

So the lower bound of the blue region is

$$\mathbf{c}_{a,2}^2 (2\pi f)^4 \sigma_\beta^2 > \frac{3}{16} \left(\frac{\pi}{\Omega} \right)^4 \sigma_\beta^4 \left[\sum_{l=1}^N \sum_{m=1}^{l-1} \sin(\phi'_m - \phi'_l) \right]^2. \quad (89)$$

The upper bound is

$$\mathbf{c}_{a,3}^2(2\pi f)^6\sigma_\beta^2 < \mathbf{c}_{a,2}^2(2\pi f)^4\sigma_\beta^2. \quad (90)$$

Substituting $\omega = 2\pi f$ and dividing by appropriate factors of Ω ,

$$\left(\frac{\omega}{\Omega}\right)^2 > \frac{\sigma_\beta}{\Omega}(\Omega^3|\mathbf{c}_{a,2}|)^{-1} \frac{\sqrt{3}}{4}\pi^2 \left| \sum_{l=1}^N \sum_{m=1}^{l-1} \sin(\phi'_m - \phi'_l) \right| \quad (91)$$

$$\frac{\omega}{\Omega} < \frac{|\mathbf{c}_{a,2}|}{|\Omega\mathbf{c}_{a,3}|} = \frac{|\Omega^3\mathbf{c}_{a,2}|}{|\Omega^4\mathbf{c}_{a,3}|}. \quad (92)$$

Beware: Ω and σ_β need to be the same for both sequences. $\mathbf{c}_{a,2}$ is calculated for to F_1 . ϕ' and $\mathbf{c}_{a,3}$ are calculated for $[\text{PLA}(2)]_1$.

[1] Harrison Ball and Michael J. Biercuk. Walsh-synthesized noise filters for quantum logic. *EPJ Quantum Technol.*, 2(1):1–45, December 2015. Number: 1 Publisher: SpringerOpen.

[2] J.P.G. van Dijk, E. Kawakami, R.N. Schouten, M. Veldhorst, L.M.K. Vandersypen, M. Babaie, E. Charbon, and F. Sestadio. Impact of Classical Control Electronics on Qubit Fidelity. *Phys. Rev. Applied*, 12(4):044054, October 2019. Publisher: American Physical Society.

[3] Harrison Ball, William D. Oliver, and Michael J. Biercuk. The role of master clock stability in quantum information processing. *npj Quantum Information*, 2(1):1–8, November 2016. Number: 1 Publisher: Nature Publishing Group.

[4] L. M. K. Vandersypen and I. L. Chuang. NMR techniques for quantum control and computation. *Reviews of Modern Physics*, 76(4):1037–1069, January 2005.

[5] K. R. Brown, A. C. Wilson, Y. Colombe, C. Ospelkaus, A. M. Meier, E. Knill, D. Leibfried, and D. J. Wineland. Single-qubit-gate error below $\mathbf{\Omega}^{10}/\mathbf{\Omega}^4$ in a trapped ion. *Phys. Rev. A*, 84(3):030303, September 2011. Publisher: American Physical Society.

[6] Emanuel Knill. Quantum computing. *Nature*, 463(7280):441–443, January 2010. Bandiera_abtest: a Cg_type: Nature Research Journals Number: 7280 Primary_atype: Comments & Opinion Publisher: Nature Publishing Group Subject_term: Information technology;Quantum physics Subject_term_id: information-technology;quantum-physics.

[7] Daniel Eric Gottesman. *Stabilizer Codes and Quantum Error Correction*. phd, California Institute of Technology, 1997.

[8] E. Knill. Quantum computing with realistically noisy devices. *Nature*, 434(7029):39–44, March 2005. Bandiera_abtest: a Cg_type: Nature Research Journals Number: 7029 Primary_atype: Research Publisher: Nature Publishing Group.

[9] Emanuel Knill, Raymond Laflamme, and Wojciech H. Zurek. Resilient quantum computation: error models and thresholds. *Proc. R. Soc. Lond. A*, 454(1969):365–384, January 1998.

[10] Kenneth R. Brown, Aram W. Harrow, and Isaac L. Chuang. Arbitrarily accurate composite pulse sequences. *Phys. Rev. A*, 70(5):052318, November 2004. Publisher: American Physical Society.

[11] J. True Merrill and Kenneth R. Brown. Progress in Compensating Pulse Sequences for Quantum Computation. In *Quantum Information and Computation for Chemistry*, pages 241–294. John Wiley & Sons, Ltd, 2014. eprint: <https://onlinelibrary.wiley.com/doi/pdf/10.1002/9781118742631.ch1>

[12] Guang Hao Low, Theodore J. Yoder, and Isaac L. Chuang. Optimal arbitrarily accurate composite pulse sequences. *Physical Review A*, 89(2):022341, February 2014.

[13] Malcolm H. Levitt. Composite pulses. *Progress in Nuclear Magnetic Resonance Spectroscopy*, 18(2):61–122, January 1986.

[14] Sami Husain, Minaru Kawamura, and Jonathan A. Jones. Further analysis of some symmetric and antisymmetric composite pulses for tackling pulse strength errors. *Journal of Magnetic Resonance*, 230:145–154, May 2013.

[15] Smita Odedra, Michael J. Thriplleton, and Stephen Wimperis. Dual-compensated antisymmetric composite refocusing pulses for NMR. *Journal of Magnetic Resonance*, 225:81–92, December 2012.

[16] S. Wimperis. Broadband, Narrowband, and Passband Composite Pulses for Use in Advanced NMR Experiments. *Journal of Magnetic Resonance, Series A*, 109(2):221–231, August 1994.

[17] Sami Husain, Minaru Kawamura, and Jonathan A. Jones. Further analysis of some symmetric and antisymmetric composite pulses for tackling pulse strength errors. *Journal of Magnetic Resonance*, 230:145–154, May 2013.

[18] Boyan T. Torosov and Nikolay V. Vitanov. Composite pulses with errant phases. *Phys. Rev. A*, 100(2):023410, August 2019. Publisher: American Physical Society.

[19] Masamitsu Bando, Tsubasa Ichikawa, Yasushi Kondo, and Mikio Nakahara. Concatenated Composite Pulses Compensating Simultaneous Systematic Errors. *J. Phys. Soc. Jpn.*, 82(1):014004, January 2013. Publisher: The Physical Society of Japan.

[20] Alexandre M. Souza, Gonzalo A. Alvarez, and Dieter Suter. Experimental protection of quantum gates against decoherence and control errors. *Phys. Rev. A*, 86(5):050301, November 2012. Publisher: American Physical Society.

[21] Kaveh Khodjasteh and Lorenza Viola. Dynamically Error-Corrected Gates for Universal Quantum Computation. *Phys. Rev. Lett.*, 102(8):080501, February 2009. Publisher: American Physical Society.

[22] C. A. Ryan, J. S. Hodges, and D. G. Cory. Robust Decoupling Techniques to Extend Quantum Coherence in Diamond. *Physical Review Letters*, 105(20):200402, November 2010.

[23] Jonathan A. Jones. Designing short robust not gates for quantum computation. *Phys. Rev. A*, 87(5):052317, May 2013. Publisher: American Physical Society.

[24] Stephen Wimperis. Iterative schemes for phase-distortionless composite 180° pulses. *Journal of Magnetic Resonance* (1969),

93(1):199–206, June 1991.

[25] Chingiz Kabytayev, Todd J. Green, Kaveh Khodjasteh, Michael J. Biercuk, Lorenza Viola, and Kenneth R. Brown. Robustness of composite pulses to time-dependent control noise. *Phys. Rev. A*, 90(1):012316, July 2014. Publisher: American Physical Society.

[26] A. Soare, H. Ball, D. Hayes, J. Sastrawan, M. C. Jarratt, J. J. McLoughlin, X. Zhen, T. J. Green, and M. J. Biercuk. Experimental noise filtering by quantum control. *Nature Physics*, 10(11):825–829, November 2014. Number: 11 Publisher: Nature Publishing Group.

[27] Xing-Long Zhen, Tao Xin, Fei-Hao Zhang, and Gui-Lu Long. Experimental demonstration of concatenated composite pulses robustness to non-static errors. *Sci. China Phys. Mech. Astron.*, 59(9):690312, July 2016.

[28] Todd J. Green, Jarrah Sastrawan, Hermann Uys, and Michael J. Biercuk. Arbitrary quantum control of qubits in the presence of universal noise. *New J. Phys.*, 15(9):095004, September 2013. Publisher: IOP Publishing.

[29] Łukasz Cywiński, Roman M. Lutchyn, Cody P. Nave, and S. Das Sarma. How to enhance dephasing time in superconducting qubits. *Phys. Rev. B*, 77(17):174509, May 2008. Publisher: American Physical Society.

[30] M. J. Biercuk, A. C. Doherty, and H. Uys. Dynamical decoupling sequence construction as a filter-design problem. *J. Phys. B: At. Mol. Opt. Phys.*, 44(15):154002, July 2011. Publisher: IOP Publishing.

[31] Gerardo A. Paz-Silva and Lorenza Viola. General Transfer-Function Approach to Noise Filtering in Open-Loop Quantum Control. *Phys. Rev. Lett.*, 113(25):250501, December 2014. Publisher: American Physical Society.

[32] Chingiz Kabytayev. *Quantum control for time-dependent noise*. PhD thesis, May 2015. Accepted: 2016-08-22T12:19:54Z Publisher: Georgia Institute of Technology.

[33] Götz S. Uhrig. Keeping a Quantum Bit Alive by Optimized π -Pulse Sequences. *Phys. Rev. Lett.*, 98(10):100504, March 2007. Publisher: American Physical Society.

[34] Götz S. Uhrig. Exact results on dynamical decoupling by π -pulses in quantum information processes. *New J. Phys.*, 10(8):083024, August 2008. Publisher: IOP Publishing.

[35] D. J. Szwer, S. C. Webster, A. M. Steane, and D. M. Lucas. Keeping a single qubit alive by experimental dynamic decoupling. *J. Phys. B: At. Mol. Opt. Phys.*, 44(2):025501, December 2010. Publisher: IOP Publishing.

[36] Michael A. Nielsen and Isaac L. Chuang. *Quantum Computation and Quantum Information*. Cambridge University Press, Cambridge; New York, 10th anniversary ed edition, 2010.

[37] D Suter and A Pines. Recursive evaluation of interaction pictures. *Journal of Magnetic Resonance (1969)*, 75(3):509–512, December 1987.

[38] Robin Blume-Kohout, John King Gamble, Erik Nielsen, Kenneth Rudinger, Jonathan Mizrahi, Kevin Fortier, and Peter Maunz. Demonstration of qubit operations below a rigorous fault tolerance threshold with gate set tomography. *Nat Commun*, 8(1):14485, February 2017. Bandiera_abtest: a Cc_license_type: cc_by Cg_type: Nature Research Journals Number: 1 Primary_atype: Research Publisher: Nature Publishing Group Subject_term: Atomic and molecular interactions with photons;Quantum information;Qubits Subject_term_id: atomic-and-molecular-interactions-with-photons;quantum-information;qubits.

[39] Qile David Su. Quasi-classical rules for qubit spin-rotation error suppression. *Eur. J. Phys.*, 42(3):035407, March 2021. Publisher: IOP Publishing.

[40] V. M. Frey, S. Mavadia, L. M. Norris, W. de Ferranti, D. Lucarelli, L. Viola, and M. J. Biercuk. Application of optimal band-limited control protocols to quantum noise sensing. *Nature Communications*, 8(1):2189, December 2017. Number: 1 Publisher: Nature Publishing Group.

[41] Virginia Frey, Leigh M. Norris, Lorenza Viola, and Michael J. Biercuk. Simultaneous Spectral Estimation of Dephasing and Amplitude Noise on a Qubit Sensor via Optimally Band-Limited Control. *Phys. Rev. Applied*, 14(2):024021, August 2020. Publisher: American Physical Society.

[42] Kaveh Khodjasteh, Jarrah Sastrawan, David Hayes, Todd J. Green, Michael J. Biercuk, and Lorenza Viola. Designing a practical high-fidelity long-time quantum memory. *Nature Communications*, 4(1):2045, June 2013. Number: 1 Publisher: Nature Publishing Group.

[43] Teerawat Chalermpusitarak, Behnam Tonekaboni, Yuanlong Wang, Leigh M. Norris, Lorenza Viola, and Gerardo A. Paz-Silva. Frame-Based Filter-Function Formalism for Quantum Characterization and Control. *PRX Quantum*, 2(3):030315, July 2021. Publisher: American Physical Society.